Low-loss arrayed waveguide grating at 2.0 µm

Eric J. Stanton*, **Nicolas Volet, and John E. Bowers**

Department of Electrical and Computer Engineering, University of California, Santa Barbara, CA 93106, USA

**estanton@ece.ucsb.edu*

Abstract: A low-loss arrayed waveguide grating operating at 2.0-µm wavelength is demonstrated with an average on-chip loss of 0.5 dB and a crosstalk per channel of −30.2 dB. These are the lowest reported values for a silicon AWG at 2.0-µm wavelength.

OCIS codes: 140.3298, 130.3120, 130.7408, 060.4510.

High-brightness light sources, detectors, and low-loss spectral beam combiners spanning wavelengths near 2-µm have recently been demonstrated [1–3]. Applications for these technologies include gas and organic molecule sensing [5,6], are promising for low-loss communication systems with hollow-core photonic-bandgap fibers [7]. An optical multiplexer is an essential device for these applications. Arrayed waveguide gratings (AWGs) have the lowest loss and crosstalk compared to other integrated spectral beam combiners, *e.g.* planar concave gratings, especially considering densely spaced wavelength channels.

A previous demonstration of AWGs near 2.0-µm wavelength [8] reported one design with 4 dB loss and a crosstalk level of −16 dB and another design with 2.15 dB loss and a crosstalk level of −12 dB. To improve the loss and crosstalk figures of merit in this work, a larger device footprint area of 3.7 mm^2 is permitted. The AWG is designed and modeled using the methodology detailed in [9]. A schematic of the AWG is shown in Fig. 1 and the corresponding design parameters are listed in Table 1.

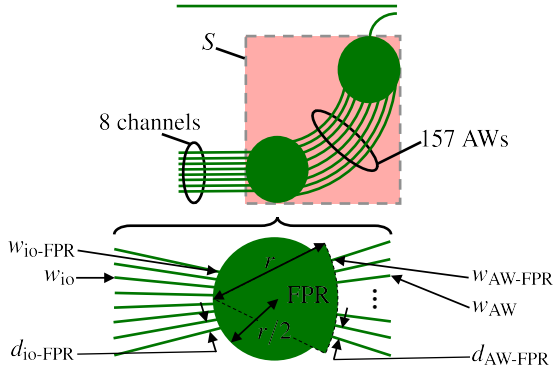

Fig. 1. AWG schematic with labeled design parameters.

Number of channels	N_{ch}	8
Number of AWs	N_{AW}	157
Rowland radius	r	241.69 µm
AW length increment	ΔL	19.56 µm
AW width	w_{AW}	1.20 µm
AW width at FPR	$w_{\text{AW-FPR}}$	1.00 µm
i/o waveguide width	w_{io}	0.80 µm
i/o waveguide width at FPR	$w_{\text{io-FPR}}$	1.40 µm
AW pitch at FPR	$d_{\text{AW-FPR}}$	1.25 µm
i/o waveguide pitch at FPR	$d_{\text{io-FPR}}$	4.20 µm
Footprint area	S	3.70 mm^2

Table 1. AWG design parameters.

The integrated devices are characterized with a fiber-coupled tunable laser (Thorlabs TLK-L1950R) capable of launching 1.88–2.02-µm wavelengths. The polarization of the laser is controlled by a rotatable fiber squeezer (Thorlabs PLC-900). A ∼5-% power tap (FONT Co.) is used to monitor the input power by connecting to an integrating sphere with an InGaAs photo-diode power sensor (Thorlabs S148C). Light is coupled through and collected from the chip via lensed fibers (OZ Optics) with AR coatings for 2-µm wavelength. The light transmitted through the AWG is measured with another integrating sphere and is normalized to the input after calibrating the power tap.

Fabrication begins with a 100-mm diameter Si-on-insulator (SOI) wafer containing a 0.50-µm thick Si layer on top of a 1.00-µm thick buried SiO_2 layer. Features are defined with deep-ultraviolet lithography and SF_6/Ar reactive ion etching to remove 0.25 µm of Si. A 4:1 mixture of sulfuric acid and hydrogen peroxide held at 80 °C strips the photoresist. A 1.00-µm thick SiO_2 layer is then sputtered to form the top cladding before dicing the wafer and polishing the facets.

Preliminary measurements are taken from one AWG device and 8 others are currently prepared for further experiments. Transmission spectra of each AWG channel are plotted in Fig. 2 by normalizing to the transmission spectra of a straight waveguide. The maximum transmittance at each wavelength from six repeated measurements of the straight

waveguide is used for this normalization. Two measurements on each AWG channel are taken for both short-to-long and long-to-short wavelength scans, where the maximum transmittance at each wavelength is used for the analysis.

Measured peak channel losses vary between a minimum of −0.08 dB and a maximum of 0.81 dB. The negative loss arises from the off- to on-chip coupling uncertainty, which will be quantified with further measurements of many straight waveguides with identical geometry. The 3-dB cumulative crosstalk averaged over all eight channels is −21.7 dB. This corresponds to a crosstalk per channel of −30.2 dB. The modeled free spectral range is 62 nm, so the adjacent transmission orders are not fully resolvable with our laser tuning range. The measured channel spacing of 1.85 nm is slightly narrower than the design of 2.0 nm. This is likely due to variation in the group effective indices of the arrayed waveguides. The 0.25-μm etch depth is only controlled within ±20 nm, which is one possible cause to this uncertainty.

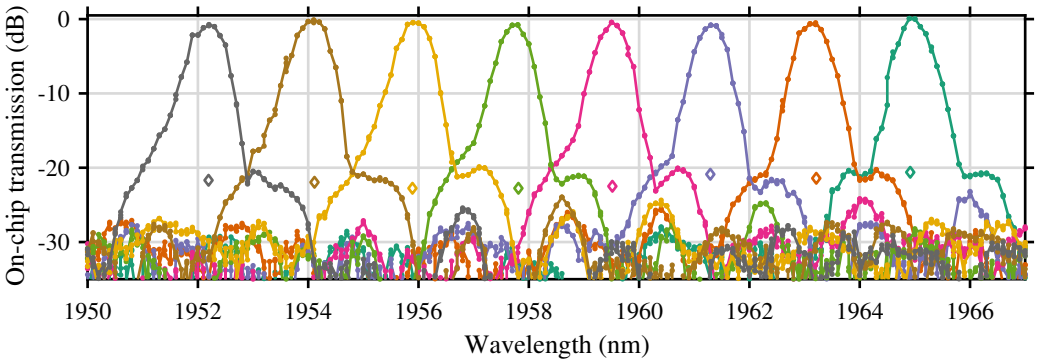

Fig. 2. Transmission spectra measured for each AWG channel shown with a different color. The 3-dB cumulative crosstalk for each channel is plotted with a diamond.

These are the lowest reported values of peak channel losses and crosstalk for an AWG at 2.0-μm wavelength. At the conference, further measurements and analysis will be added to these preliminary measurements to better understand the device performance. Regardless, this AWG design has already been demonstrated as suitable for applications demanding ultra-low loss spectral beam combining, such as for multi-spectral lasers, sensitive spectroscopy, and low-loss communication systems near 2.0-μm wavelength.

This research is funded by the Office of Naval Research (ONR) contract N00014-13-C-0147 and N. V. acknowledges support from the Swiss National Science Foundation. The authors thank M. L. Davenport for fabrication advice.

References

1. A. Spott *et al.*, "Heterogeneously integrated 2.0 μm CW hybrid silicon lasers at room temperature," Opt. Lett. **40**, 1480–1483 (2015).
2. R. Wang *et al.*, "2 μm wavelength range InP-based type-II quantum well photodiodes heterogeneously integrated on silicon photonic integrated circuits," Opt. Express **23**, 26834–26841 (2015).
3. R. Wang *et al.*, "Heterogeneously integrated III-V-on-silicon 2.3x μm distributed feedback lasers based on a type-II active region," Appl. Phys. Lett. **109**, 221111 (2016).
4. N. Volet *et al.*, "Semiconductor optical amplifier at 2.0-μm wavelength on silicon," submitted to Laser Photon. Rev. (2016).
5. S. Ishii *et al.*, "Coherent 2 μm differential absorption and wind lidar with conductively cooled laser and two-axis scanning device," Appl. Opt. **49**, 1809–1817 (2010).
6. N. V. Alexeeva and M. A. Arnold, "Near-infrared microspectroscopic analysis of rat skin tissue heterogeneity in relation to noninvasive glucose sensing," J. Diabetes Sci. Technol. **3**, 219–232 (2009).
7. Y. Chen *et al.*, "Multi-kilometer long, longitudinally uniform hollow core photonic bandgap fibers for broadband low latency data transmission," J. Lightw. Technol. **34**, 104–113 (2016).
8. E. Ryckeboer *et al.*, "Silicon-on-insulator spectrometers with integrated GaInAsSb photodiodes for wide-band spectroscopy from 1510 to 2300 nm," Opt. Express **21**, 6101–6108 (2013).
9. E. J. Stanton *et al.*, "Low-loss arrayed waveguide grating at 760 nm," Opt. Lett. **41**, 1785–1788 (2016).